

# Active Control of Microcapsules in Artificial Blood Vessel by producing Local Acoustic Radiation Force

Kohji Masuda, *Member, IEEE*, Ryusuke Nakamoto, Yusuke Muramatsu, Yoshitaka Miyamoto, Keri Kim and Toshio Chiba

**Abstract**— Micrometer-sized microcapsules collapse upon exposure to ultrasound. Use of this phenomenon for a drug delivery system (DDS), not only for local delivery of medication but also for gene therapy, should be possible. However, enhancing the efficiency of medication is limited because capsules in suspension diffuse in the human body after injection, since the motion of capsules in blood flow cannot be controlled. To control the behavior of microcapsules, acoustic radiation force was introduced. We detected local changes in microcapsule density by producing acoustic radiation force in an artificial blood vessel. Furthermore, we theoretically estimated the conditions required for active path selection of capsules at a bifurcation point in the artificial blood vessel. We observed the difference in capsule density at both in the bifurcation point and in alternative paths downstream of the bifurcation point for different the acoustic radiation forces. Also we confirmed the microcapsules are trapped against flow with the condition when the acoustic radiation force is more than fluid resistance of the capsules. The possibility of controlling capsule flow towards a specific point in a blood vessel was demonstrated.

## I. INTRODUCTION

THE phenomenon that microcapsules or microbubbles of micrometer size collapse upon exposure to ultrasound near their resonance frequency has been identified as a basis for a physical drug delivery system (DDS) [1-3]. To minimize side effects, medication should only affect the target area, not other parts of the human body. Although the majority of its recent research on DDSs has been focused on gene transduction using gene vectors, this method takes time and development is costly. While the lifetime of the microbubbles is several minutes, the microcapsules, which can contain a specific drug inside a shell, are suitable for use with various types of medication. Furthermore, microcapsules are easily detected [4] and actuated [5,6] by ultrasound. The distribution of capsules inside the body is easily determined by echogram (B-mode image) because the brightness of an echogram varies depending on capsule density. We have developed software to detect local changes

in capsule density using the variation in brightness of an echogram [7]. Figure 1 shows a microscope image of F-80E microcapsules (Matsumoto Oil), which we used in this work.

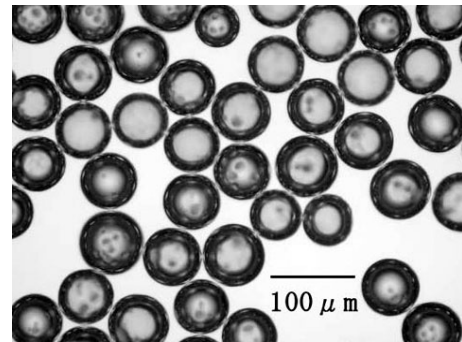


Fig.1. Microscope image of F-80E microcapsules.

However, because of the diffusion of capsules after injection, it is difficult to enhance the efficiency of medication. If the behavior of capsules could be controlled, the amount of medication required would be minimized. Microbubbles aggregate in water owing to Bjerknes forces, [8,9] which are produced by an ultrasound pressure gradient and oscillation of the diameter of the microbubbles. Since the oscillation of microcapsules is smaller than that of microbubbles, because of the microcapsule shell, a microcapsule is thought to receive an acoustic radiation force [10-12] and be propelled by acoustic propagation. In this paper, we describe our attempt for active path selection of microcapsules in an artificial blood vessel by acoustic radiation force.

## II. THEORY

Assuming spherical microcapsules, an acoustic radiation force [10] acts to propel the capsules in the direction of acoustic propagation as per the following equation:

$$F_{ac} = \frac{4}{3}\pi R_0^3 A \frac{P^2}{\rho c^2}, \quad (1)$$

where  $R_0$  is the average capsule radius,  $P$  is the sound pressure, and  $\rho$  is the density of the medium.  $A$  is a constant which is derived from  $\rho$  and the density of capsules.

When the microcapsules are placed in flow, a capsule should receive a flow resistance  $F_d$  as per the following equation:

$$F_d = 6\pi R_0 \mu u_r, \quad (2)$$

Manuscript received April 7, 2009. This work was supported in part by Health Labor Sciences Research Grant 200813004A.

Kohji Masuda, Ryusuke Nakamoto and Yusuke Muramatsu are with Graduate School of Bio-Applications and Systems Engineering, Tokyo University of Agriculture and Technology, Koganei, Tokyo, 184-8588 Japan (e-mail: [masuda\\_k@cc.tuat.ac.jp](mailto:masuda_k@cc.tuat.ac.jp)).

Yoshitaka Miyamoto is with School of Medicine, Nagoya University, Nagoya, 466-8550 Japan.

Keri Kim and Toshio Chiba is with National Center for Child Health and Development, Tokyo, 157-8535 Japan

where  $u_r$  is the velocity caused by the acoustic radiation force and  $\mu$  is the viscosity coefficient of the medium. Thus, if ultrasound is directed at a microcapsule in flow, and the acoustic radiation force is greater than the flow resistance, the trajectory of the capsule is curved, as shown in Fig.2.

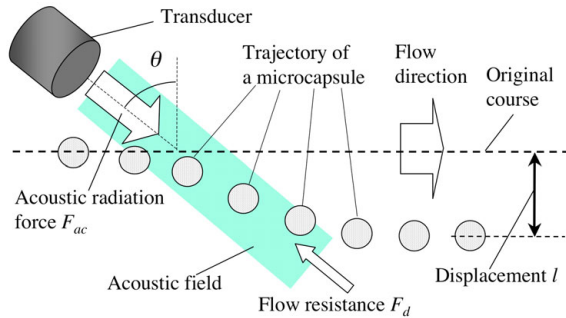


Fig.2. Trajectory of microcapsule in flow under ultrasound emission.

When microcapsules pass through an acoustic field where the sound pressure is higher than that at other areas, capsules are propelled away from their original course. At larger value of angle  $\theta$  in Fig.2, a capsule passes through the acoustic field for a longer period causing a larger displacement from the original course. In Fig.2, although the shape of the acoustic field is expressed as a square, it is dependent upon the transducer and should be measured before the calculation of theoretical displacement.

### III. EXPERIMENTS

#### A. Evaluation of active path selection of microcapsules

We used the above-mentioned F-80E microcapsule, which has a shell made of polyvinyl chloride (PVC), a specific gravity of 0.0225, and an average diameter of 99.2  $\mu\text{m}$ . It contains isobutene inside and is stable in room temperature. We selected only those microcapsules with a diameter in the range from 65 to 73  $\mu\text{m}$  because of the limited magnification of the microscope. This size of capsule, of course, is not suitable for use *in vivo*, but is useful for confirming the fundamental behavior of capsules before minimizing them in the future experiments.

We also have prepared an artificial blood vessel made of polyethylene glycol (PEG), including a Y-form bifurcation as shown in the schematic view of Fig.3. The external size was 50 x 80 x 10  $\text{mm}^3$  and the inner diameter of the paths was 2 mm. The blood vessel was placed in the bottom of a water tank, which was filled with water. Because the acoustic impedance of PEG is similar to that of water, the energy of ultrasound in water reaches the path with high efficiency. Using an inverted microscope (Leica, DMRIB), optical images of the observed areas 1 and 2 indicated in Fig.3 were recorded independently.

Figure 4 shows the relationship between focal areas of ultrasound and the bifurcation in the observed area 1. The axis of the transducer was set at 50 degrees counterclockwise to the  $x$ -axis and  $\theta$  deg clockwise to the

$z$ -axis to prevent physical interference between the transducer and the edge of the water tank. The transducer included a concave ceramic disc with a diameter of 25 mm. Ultrasound was emitted by amplifying a sinusoidal signal of 1 MHz to an amplitude of 160 kPa where the focal area of ultrasound is created in 60 mm from the surface of the transducer with a half width of sound pressure of 8 mm.

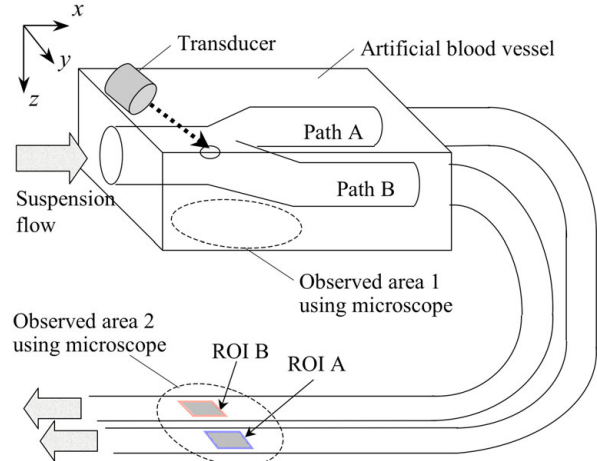


Fig.3. Configuration of artificial blood vessel, transducer, and two observed areas using microscope to evaluate active path selection of microcapsules.

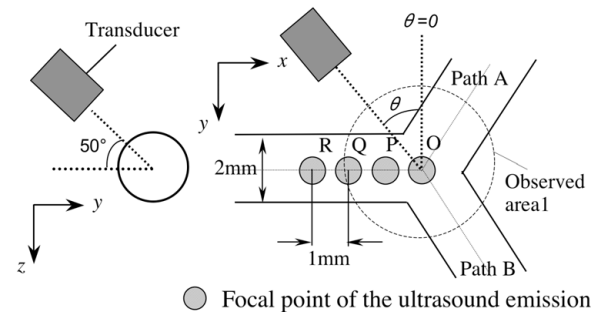


Fig.4. Relationship between focal points of ultrasound and the bifurcation in the observed area 1.

Defining point O as the intersection of the three paths in Fig.4, the points P, Q, and R indicate points 1, 2, and 3 mm upstream from O, respectively. We observed the behavior of capsules in the observed area 1 upon the injection of a capsule suspension at a flow velocity of 100 mm/s. When ultrasound was emitted, more capsules entered path B than path A, whereas no significant difference was observed without ultrasound emission. Figure 5 shows the comparison of microscope images of the observed area 1 before and after the capsule suspension was injected and ultrasound was focused at point Q. Since amount of capsules were observed as a shadow, the possibility of active path selection of capsules was indicated. Here we confirmed that the capsules were not destroyed by the ultrasound since the frequency used was far from the resonance frequency of the capsules.

To evaluate the number of capsules that passed through each path, we extended the two paths using semitransparent tubes and established an observed area 2, where both paths were observable in a single view, as shown in Fig.3.

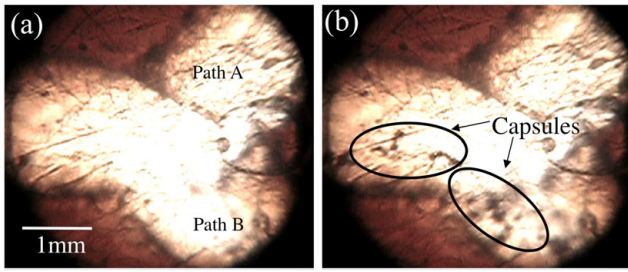


Fig.5. Comparison of microscope images of observed area 1 (a) before and (b) after injection of capsule suspension with ultrasound emission.

Figure 6 shows microscope images of the observed area 2, which were captured using a high-speed camera Phantom-V4.2 (Nobitec Co., Ltd., Japan) with an interval time of 2 ms, upon injection of a capsule suspension under the same conditions as for Fig.5. Individual microcapsules can be distinguished.

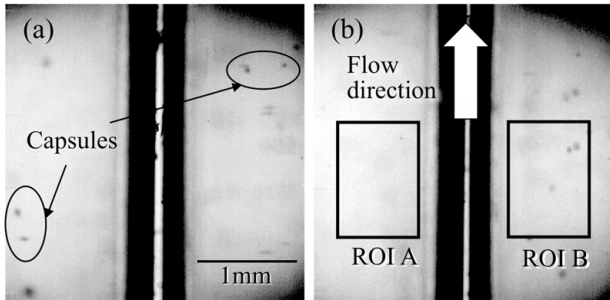


Fig.6. Microscope images of observed area 2 taken at 500 fps after injection of capsule suspension (a) without and (b) with ultrasound emission.

To measure the number of microcapsules, we established two square regions of interest in each path (ROIs A and B) and calculated the average brightness. The brightness of a region decreases depending on the number of capsules present. Thus, we defined the shadow index  $\sigma$  using the following equation to determine the number of capsules in each ROI:

$$\sigma = \left( REF - \sum_x \sum_y f(x,y) \right) / REF, \quad (3)$$

where  $f$  is the brightness of the ROI and  $REF$  is the summation of brightness in the absence of capsules in the ROI. Then, we confirmed the relation between shadow index and capsule density. A capsule suspension was passed through the ROI without ultrasound and the average of the shadow index for 15 frames (duration 30 ms) was calculated for various flow velocities. When capsule density was 0.15-0.25 g/L, significant changes in density were detected [13].

#### B. Trapping microcapsules against flow

To observe the behavior of microcapsules if the acoustic radiation force propels microcapsules against flow, we have prepared the artificial blood vessel including a straight path as the schematic view, as shown in Fig.7. The external size is  $55 \times 80 \times 10 \text{ mm}^3$  and the inner diameter of the path is 2

mm. It is placed in the bottom of water tank, which is filled with water. By using an optical microscope (KH-7700, Omron, Japan), behavior of microcapsules is observed and recorded.

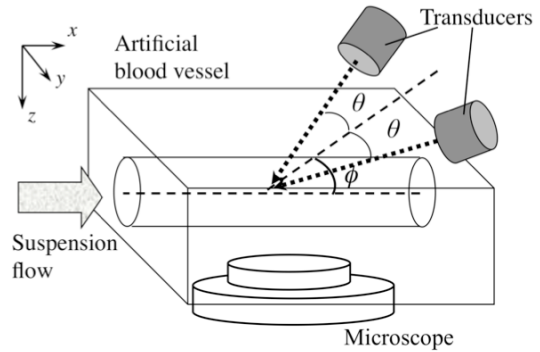


Fig. 7. Schematic view of the experiment to trap capsules.

We introduced two transducers, which were the same used for active path selection, to be focused at the identical point with their angle and  $2\theta$  as shown in Fig.7. The plane which includes axes of the transducers was set  $\phi = 50$  deg to prevent physical intervention between the transducer and an edge of the water tank. Ultrasound was emitted by amplifying sinusoidal signal to the amplitude from 110 to 210 kPa.

We observed the focal area under emission of sinusoidal ultrasound with frequency of 1 MHz and angle  $\theta$  of 30 deg. Fig.8 shows a microscope image of the area where capsules are trapped by ultrasound of 175 kPa in the middle of the path against flow of 40 mm/s. Thus we established the ROI of  $3.2 \times 1.6 \text{ mm}^2$  in the image to measure occupied area by trapped microcapsules, which was similar evaluation to the above-mentioned shadow index.

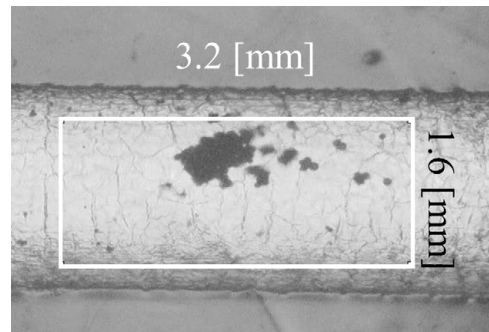


Fig. 8. A microscope image where microcapsules are trapped against flow at the focused area under ultrasound emission (210kPa, 1MHz)

## IV. RESULTS

### A. Evaluation of active path selection of microcapsules

We measured the shadow indices in two ROIs upon emission of sinusoidal ultrasound with a frequency of 1 MHz, a flow velocity of 100 mm/s, and a capsule density of 0.2 g/L, where ultrasound was focused at points O, P, Q, and R shown in Fig.4. Figure 9 shows the difference in shadow indices between ROIs A and B versus the angle of

ultrasound emission  $\theta$  for four focal points. Because the difference was calculated by subtracting the shadow index of ROI A from that of ROI B, a positive value for the difference indicates that more capsules passed through path B than path A. When the focal point was at O, no significant difference was observed. Upstream from O, clear capsule selection to path B was confirmed at angles of emission between 30 and 60 degrees. The optimum condition for active path selection in the experiment was at an angle of 50 degrees at focal point Q.

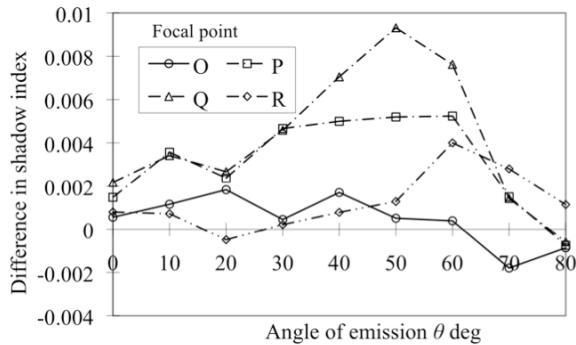


Fig.9. Shadow index difference between two ROIs versus angle of emission with ultrasound of 1 MHz, 160 kPa, and flow velocity of 100 mm/s.

We repeated the same experiment at a flow velocity of 100 mm/s. When the sound pressure was less than 120 kPa, there was no difference between the two ROIs. However, the value of shadow index in ROI B increased in proportion to the sound pressure at more than 140 kPa. More than 90% of capsules entered to path B when the sound pressure was more than 160 kPa. Next, when we fixed the sound pressure to 160 kPa, the value of shadow index in path B decreased in proportion to the flow velocity. The range of flow velocity for clear path selection appears to be less than 150 mm/s. When the flow velocity was more than 200 mm/s, path selection did not function, which we assume is because the capsules pass through the acoustic field without receiving sufficient acoustic radiation force.

From these results, the sound pressure, focal point, and flow velocity should be considered to realize active path selection of microcapsules. When the focal point of ultrasound emission is at the bifurcation point itself, active path selection of capsules is not realized. In the present experiment, the inner diameter of the path was 2 mm, so a 1 mm displacement was necessary from the beginning of the acoustic field to the bifurcation point, as shown in Fig.2.

#### B. Trapping microcapsules against flow

By referring the above condition, we recorded the microscope image when the amount of capsules is saturated under ultrasound emission. Then we calculated the average area occupied by trapped microcapsules in the ROI through the experiment. We attempted the experiment in various flow velocities and sound pressures. Fig.10 shows the average area occupied by microcapsules versus flow velocity with parameter of sound pressure. We confirmed the similar

tendency of the active path selection when the flow velocity was fixed and the sound pressure was increased, average area occupied by microcapsules was increased. If the sound pressure was fixed, the average area was decreased in proportion to the flow velocity.

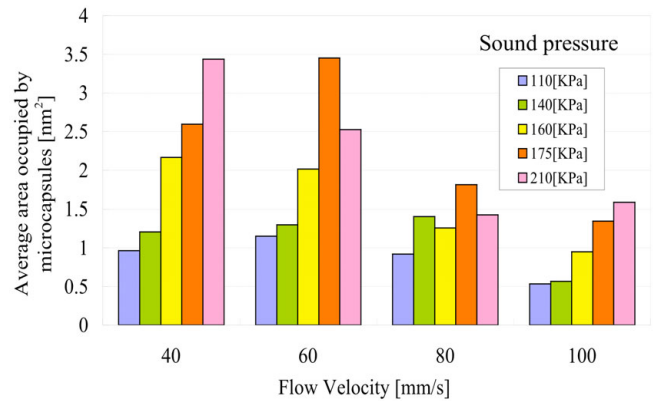


Fig.10. Average area occupied by trapped microcapsules in the ROI of microscopic image, versus flow velocity with parameters of sound pressure.

## V. CONCLUSIONS

In this study, we realized active control of microcapsules in an artificial blood vessel by acoustic radiation force. We confirmed that capsules with a diameter between 65 and 73  $\mu\text{m}$  were directed into the desired path and were not destroyed by ultrasound of a sinusoidal signal of 1 MHz. Also we confirmed that capsules were trapped against flow when the flow velocity was less than that the active path selection was observed. We are going to continue our research by varying other parameters of this experiment before applying *in vivo* experiment. For further analysis, the precise conditions necessary to realize active control of capsules in a complicated shape of blood vessel should be elucidated.

## REFERENCES

- [1] M. Watanabe, K. Chihara, K. Shirae, K. Ishihara, and A. Kitabatake: Jpn. J. Appl. Phys. 30, (1991) Suppl.1, 241-243.
- [2] K. Okada, N. Kudo, K. Niwa, and K. Yamamoto: J. Med. Ultrason. 32 (2005) 3-11.
- [3] D. Koyama, A. Osaki, W. Kiyan, and Y. Watanabe: IEEE Trans. Ultrason. Ferroelect. Freq. Control, 53 (2006) 1314-1321.
- [4] K. Ishihara, K. Yoshii, K. Chihara, K. Masuda, K. Shirae, and T. Furukawa: Proc. IEEE Ultrasonic Symp., 1992, p.1277-1280.
- [5] Y. Yamakoshi: Jpn. J. Appl. Phys. 40 (2001) 1526-1527.
- [6] K. Wei, D. M. Skyba, C. Firsche, A. R. Jayaweera, K. R. Lindner, and S. Kaul: J. Am. Coll. Cardiol., 29 (1997) 1081-1088.
- [7] H. Yoshikawa, T. Azuma, K. Sasaki, K. Kawabata, and S. Umemura: Jpn. J. Appl. Phys. 45 (2006) 4754-4760.
- [8] H. Mitome: Jpn. J. Appl. Phys. 40 (2001) 3484-3487.
- [9] Y. Yamakoshi and T. Miwa: Jpn. J. Appl. Phys. 47 (2008) 4127-4131.
- [10] T. Kozuka, K. Yasui, T. Tuziuti, A. Towata, and Y. Iida: Jpn. J. Appl. Phys. 47 (2008) 4336-4338.
- [11] T. Lilliehorn, U. Simu, M. Nilsson, M. Almqvist, T. Stepinski, T. Laurell, J. Nilsson, and S. Johansson: Ultrasonics 43 (2005) 293-303.
- [12] H. Zheng, P.A. Dayton, C. Caskey, S. Zhao, S. Qin and K.W. Ferrara: Ultrasound in Medicine and Biology, 33 (2007) 1978-1987
- [13] K. Masuda, Y. Muramatsu, R. Nakamoto, S. Ueda, Y. Nakayashiki, and K. Ishihara: Jpn. J. Appl. Phys. 48 (2009) in press.